Dynamics of Soft Nanomaterials Captured by Transmission Electron Microscopy in Liquid Water

Maria T. Proetto,[†] Anthony M. Rush,[†] Miao-Ping Chien,[†] Patricia Abellan Baeza,[‡] Joseph P. Patterson,[†] Matthew P. Thompson,[†] Norman H. Olson,[†] Curtis E. Moore,[†] Arnold L. Rheingold,[†] Christopher Andolina,[§] Jill Millstone,[§] Stephen B. Howell,[⊥] Nigel D. Browning,[‡] James E. Evans,[‖] and Nathan C. Gianneschi*,[†]

[†]Department of Chemistry & Biochemistry and [⊥]Moores Cancer Center, University of California, San Diego, La Jolla, California 92093, United States

[‡]Fundamental Computational Sciences Directorate and [‖]Environmental Molecular Sciences Laboratory, Pacific Northwest National Laboratory, Richland, Washington 99354, United States

[§]Department of Chemistry, University of Pittsburgh, Pittsburgh, Pennsylvania 15260, United States

S *Supporting Information*

ABSTRACT: In this paper we present *in situ* transmission electron microscopy of synthetic polymeric nanoparticles with emphasis on capturing motion in a solvated, aqueous state. The nanoparticles studied were obtained from the direct polymerization of a Pt(II)-containing monomer. The resulting structures provided sufficient contrast for facile imaging *in situ*. We contend that this technique will quickly become essential in the characterization of analogous systems, especially where dynamics are of interest in the solvated state. We describe the preparation of the synthetic micellar nanoparticles together with their characterization and motion in liquid water with comparison to conventional electron microscopy analyses.

Nanoparticles of all types are routinely imaged as static objects by electron microscopy (EM) methods. However, since soft matter is often exclusively composed of elements with low atomic number ($Z < 16$), image contrast using EM techniques is frequently low. To resolve soft matter using EM, samples are generally stained with heavy metals or halides. This staining process along with incident high energy electrons can cause damage or physical distortion during the process of characterization itself.[1] Cryo-transmission electron microscopy (cryo-TEM) is sometimes favored because the technique allows materials to be rapidly immobilized in vitreous ice, and hence imaged in what is widely considered a proxy for their native, solution-phase state. Despite the valuable and complementary information obtained using a combination of these imaging techniques, such an approach is not ideal for the observation of particle dynamics in real-time since either process of drying or freezing completely prohibits native motion. Therefore, a third approach enabling the imaging of synthetic nanoscale particles in their natural, solvated state is necessary and would serve as a complementary method to both dry-state and cryo-TEM. *In situ* liquid TEM, has seen a strong resurgence across many fields including inorganic nanomaterial nucleation and growth from solution,[2−4] electrochemistry,[5,6] and biology.[7−9] The first example using an *in situ* liquid environmental holder was

demonstrated in 1935.[10,11] However, with the advent of reproducible cryo-TEM,[12] where near-atomic resolution was readily achievable, the use of *in situ* TEM waned. In recent times, advancements in microfabrication techniques and EM technology including low-dose spherical aberration correction[13] have enabled atomic resolution imaging of immobilized inorganic nanoparticles[2,14] and analyses of their dynamics,[3,15−21] suggesting that *in situ* imaging quality is now limited by the sample instead of the microscope platform. We believe this fact provides a timely opportunity for imaging the dynamics of soft, organic materials on the nanometer length scale. Here we describe a pilot study aimed at demonstrating the feasibility of such an imaging strategy for capturing the motion of synthetic soft matter at the nanoscale.

Soft materials are particularly interesting candidates for *in situ* imaging due to the fact that in solution their morphology can be manipulated by a broad range of stimuli[22] including metals,[23] pH,[24] temperature,[25] light,[26] redox chemistry,[27] ultrasound,[28] DNA hybridization,[29] and enzymes.[30] Furthermore, organic liposomes and synthetic polymer vesicles have been imaged via *in situ* TEM but only as stationary, static objects,[16,31,32] which have sometimes appeared crenated as if dehydrated.[31] However, to our knowledge there are no examples using this imaging technique to capture the dynamics or motion of soft organic materials at the nanometer length scale. This constitutes a tremendous gap in our capabilities despite the fact that other techniques including dynamic light scattering (DLS), small-angle neutron scattering (SANS), small-angle X-ray scattering (SAXS), and nanoparticle tracking analysis (NTA) are capable of analyzing size and morphology of nanomaterial populations in solution in real time. However, these well-known techniques do not allow for the direct visualization of such changes for individual particles with nanometer resolution.

The studies presented herein were conducted with polymeric micellar nanoparticles obtained from amphiphilic block copolymers in which the hydrophobic block is the result of

the direct polymerization of the heavy-metal-containing norbornyl monomer, which was designed as a square planar Pt(II) complex polymerizable via ring-opening metathesis polymerization (ROMP) (Figure 1).[33] The final Pt(II)-core micelles were obtained by dissolving the resulting polymers in DMF and slowly dialyzing into water over 2 days. DLS and NTA analyses reveal nanoparticles in the 120 nm diameter range (Figures S1 and S2 in the Supporting Information). These systems were chosen for the studies presented here, as micelles loaded with the covalently attached platinum chelate provided exceptional contrast in TEM, eliminating the need for staining during sample preparation (as seen clearly in Figures 1a and S3). In addition, images of unstained particles characterized by STEM-EDS confirm the presence of platinum (Figures 1b and S4−S6).

As an initial demonstration of the power of this technique in imaging soft nanoparticles and their motion in their native solvated state, we present a series of multi-minute movies (Supporting Information) and corresponding screen shots (Figures 2 and 3). Single frames of one of the movies are shown in Figure 2, where the motion of the soft nanoparticles in the liquid cell can be clearly observed. Two different particle arrangements captured *in situ* are highlighted: a dimeric and a trimeric species undergoing motion within the field of view. Following particles A and B, we can identify them in contact
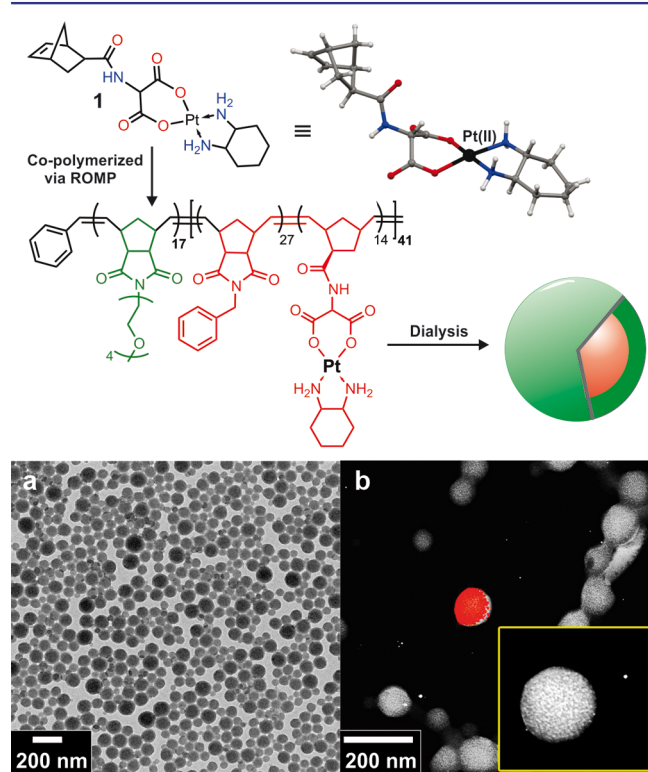

Figure 1. Preparation of micellar nanoparticles consisting of a Pt(II)-labeled core. Top: Structure of Pt(II)-norbornyl monomer (**1**), X-ray crystal structure, and amphiphilic block copolymer. Dialysis from DMF into water yielded high contrast, spherical micelles with Pt(II)-labeled cores (red). Bottom: (a) Conventional dry-state TEM of unstained micelles. (b) STEM−energy-dispersive X-ray spectroscopy (STEM-EDS) elemental map indicating platinum overlaid on the corresponding STEM−high-angle annular dark-field microscopy (HAADF) image. Inset: zoomed STEM-HAADF image of a particle (yellow box has horizontal dimension of 200 nm).

with each other (red and blue dots indicate particle centers) undergoing varied motion within the imaged field during the time course shown. A similar situation can be observed for particles C, D, and E, where the motion of the trimeric system of particles (yellow, pink, and green dots indicating particle centers) is greater than that observed for surrounding particles. Velocity vs time plots clearly demonstrate limited motion for these particles; for example an average velocity of 27 nm/s for particle A is observed. When compared to bulk Brownian motion detected for the same particles by NTA (28 000 nm/s), we conclude that the particles are temporarily adsorbed, but not irreversibly fixed, to the silicon nitride window. Temporal resolution is a key factor when imaging particles in motion. In this experiment a maximum frame rate of 25 frames/s was used, and therefore it would not be possible to observe particles undergoing bulk Brownian motion. Temporal resolution down to approximately 10 ns is now possible with dedicated dynamic TEM (DTEM) instruments that use single shot, short pulses of electrons to image materials in real-time.[34−36] However, for standard TEM instruments this is not possible, and therefore it is necessary to understand the dynamics of particles in the liquid cell in terms of interactions with the silicon nitride surface, the aqueous solution and with other particles. In the simplest case one can imagine particles undergoing a surface attachment/detachment process whereby particle motion occurs when detached and high-resolution particle observation is possible only when they reattach. This process can be inferred from the velocity "jumps" observed in Figure 2.[21]

In another experiment, to further elucidate these types of dynamic interactions, three particles were tracked within a shorter time frame (Figure 3; see Supporting Information Movie_Fig3.mov for zoom-out and Movie_S2_Fig3.avi, starting at the frame shift at 52 s, for full time course). This tracking analysis reveals concerted motion between the three particles. It is interesting to note that these particles seem to undergo cooperative motion. This could be due to beam induced charging effects between particles, charging effects induced from solution, or charging effects from the silicon nitride surface itself. It appears that these sorts of Coulombic interactions operate on the second to minute time scale. Recognizing and controlling these types of interactions will be of crucial importance in developing *in situ* imaging of nanomaterials in the immediate future. Furthermore, irradiation by the electron beam plays a key role in the behavior of materials inside the imaging cell itself.[37,38] Understanding the rate and impact of this type of damage will be key in developing new design parameters for these types of analyses. In this instance, micellar nanoparticles appear to be physically stable against electron beam damage for several minutes, after which the particles appear to agglomerate. This suggests that time-resolved observations of organic nanoparticles undergoing stimuli responsive dynamics on the seconds to minutes time scale should be possible. Therefore, the study presented herein serves as a necessary part of ongoing work to determine the threshold under which imaging experiments can be used to glean meaningful information for soft materials and their dynamics.

Having analyzed particle dynamics via *in situ* TEM, we sought to compare observed morphologies with standard and cryogenic TEM methods. Therefore, the materials were characterized by dry-state TEM without stain (Figures 1 and S8) and with uranyl acetate staining (Figure S9). Furthermore, cryo-TEM, similar to observations for *in situ* and unstained
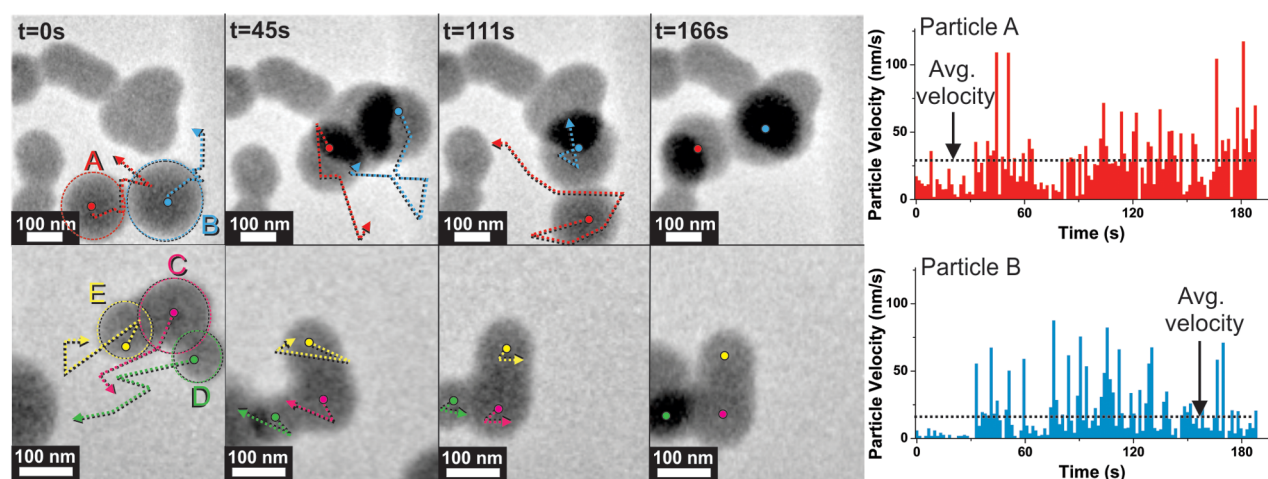
Figure 2. Left: Sequential snapshots from *in situ* TEM movies of nanoparticles in liquid water at times shown. Five particle centers (A–E) were selected, with arrows indicating particle motion during the time lapse. Right: Velocity vs time plots for particles A and B highlighting distinct motion for each of the two connected particles. The dotted line in each graph represents the average velocity for each particle during the imaged time lapse (average velocity for particle A = 27.5 nm/s, for particle B = 18.0 nm/s). See Figure S7 for velocity plots for particles C, D, and E. Motion and velocity analyses were performed using ImageJ with MTrackJ plugin. For related movies see Supporting Information: Movie_-Fig2_Particles_AB.mov, Movie_Fig2_Particles_CDE.mov, and Movie_S1_Fig2.avi. Images captured in silicon nitride *in situ* cells with 50 nm thick windows.
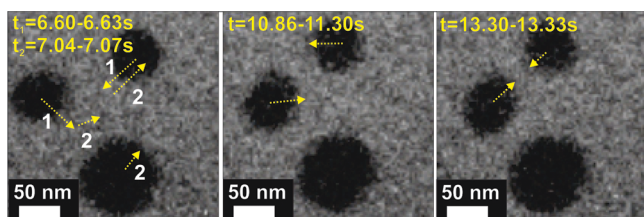

Figure 3. Screen shots from an *in situ* liquid stage movie. Arrows indicate direction of motion between the times indicated (see Supporting Information Movie_Figure 3.mov).

TEM experiments, reveals high contrast for this class of particle (Figures 4 and S10). Image analysis of particles (Figures S8–S11) shows a small variation in size but overall we observed Gaussian fits for each technique showing maximum intensities centered at ~90 nm (see Figure S12). *In situ* measurements reveal what appears to be a tighter distribution of sizes; however, analyses of *in situ* samples were only conducted on particles that were obviously spherical from snapshots, limiting the population size that could be analyzed in this initial study. It is important to note this as it highlights an inherent feature of
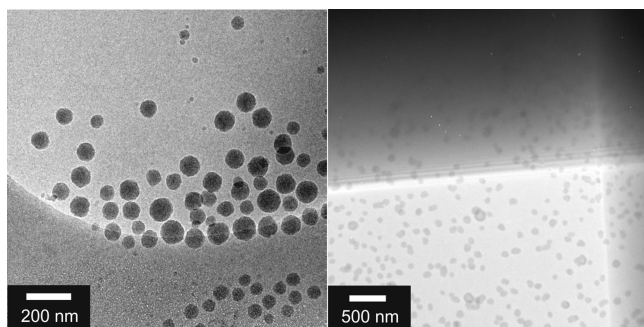
the approach, namely, that multiple particles can occupy a similar position within the field of view but differ with respect to the vertical axis through the sample and therefore may appear as aggregates (Figure 4). This is clearly observed in movies that reveal sets of particles passing over each other in solution confirming they are separate species overlaid in the *z*-axis; for example, this is clearly observed in Figure 2, with particles A and B. From these parallel analyses we can conclude that *in situ* TEM is capable of capturing soft nanoparticle morphologies in a manner comparable to more traditional techniques, with the added capability of allowing one to image particles in motion.

In summary, we have demonstrated that *in situ* TEM is a viable approach for imaging the motion of organic, polymeric soft nanomaterials in liquid water. In terms of soft materials, *in situ* TEM should become a new standard to add to the suite of microscopy methods employed to interrogate structure. Furthermore, with an understanding of operational parameters and limitations of the materials in hand, the technique will prove to become a unique tool for high resolution characterization of *dynamic* systems. Finally, we note that these particles, loaded with a heavy metal for contrast, made for an initial, straightforward imaging study *in situ*. However, we do not believe that this heavy metal loading strategy is a prerequisite, and we are currently screening other organic materials and dynamic, switchable systems for their ability to be imaged. These studies are currently underway and we aim to describe these in due course.

■ ASSOCIATED CONTENT

Ⓢ Supporting Information

Detailed materials and sample preparation, together with additional images and movie files (key to file names: ja408513m_si_002.mov = Movie_Fig2_Particles_AB.mov; ja408513m_si_003.mov = Movie_Fig2_Particles_CDE.mov; ja408513m_si_004.mov = Movie_Fig3.mov; ja408513m_-si_005.mov = Movie_S1_Fig2.avi; ja408513m_si_006.mov =

Figure 4. Comparison of Pt(II)-core micelles visualized via (left) cryo-TEM and (right) *in situ* TEM showing dispersed particles for each method.

1164

dx.doi.org/10.1021/ja408513m | *J. Am. Chem. Soc.* 2014, 136, 1162–1165

Movie_S2_Fig3.avi). This material is available free of charge via the Internet at http://pubs.acs.org.

■ AUTHOR INFORMATION

Corresponding Author
ngianneschi@ucsd.edu

Notes
The authors declare no competing financial interest.

■ ACKNOWLEDGMENTS

■ REFERENCES

(1) Egerton, R. F. *Ultramicroscopy* **2013**, *127*, 100.
(2) Evans, J. E.; Jungjohann, K. L.; Browning, N. D.; Arslan, I. *Nano Lett.* **2011**, *11*, 2809.
(3) Woehl, T. J.; Evans, J. E.; Arslan, I.; Ristenpart, W. D.; Browning, N. D. *ACS Nano* **2012**, *10*, 8599.
(4) Zheng, H.; Smith, R. K.; Jun, Y. W.; Kisielowski, C.; Dahmen, U.; Alivisatos, A. P. *Science* **2009**, *324*, 1309.
(5) Williamson, M. J.; Tromp, R. M.; Vereecken, P. M.; Hull, R.; Ross, F. M. *Nat. Mater.* **2003**, *2*, 532.
(6) White, E. R.; Singer, S. B.; Augustyn, V.; Hubbard, W. A.; Mecklenburg, M.; Dunn, B.; Regan, B. C. *ACS Nano* **2012**, *6*, 6308.
(7) Sugi, H.; Minoda, H.; Inayoshi, Y.; Yumoto, F.; Miyakawa, T.; Miyauchi, Y.; Tanokura, M.; Akimoto, T.; Kobayashi, T.; Chaen, S.; Sugiura, S. *Proc. Natl. Acad. Sci. U.S.A.* **2008**, *105*, 17396.
(8) Peckys, D. B.; Veith, G. M.; Joy, D. C.; de Jonge, N. *PLoS One* **2009**, *4*, e8214.
(9) Evans, J. E.; Jungjohann, K. L.; Wong, P. C.; Chiu, P. L.; Dutrow, G. H.; Arslan, I.; Browning, N. D. *Micron* **2012**, *43*, 1085.
(10) Marton, L. *Bull. Acad. R. Med. Belg.* **1935**, *21*, 600.
(11) Parsons, D. F. *Science* **1974**, *186*, 407.
(12) Adrian, M.; Dubochet, J.; Lepault, J.; McDowall, A. W. *Nature* **1984**, *308*, 32.
(13) Evans, J. E.; Hetherington, C.; Kirkland, A.; Chang, L. Y.; Stahlberg, H.; Browning, N. *Ultramicroscopy* **2008**, *108*, 1636.
(14) Jungjohann, K. L.; Evans, J. E.; Aguiar, J. A.; Arslan, I.; Browning, N. D. *Microsc. Microanal.* **2012**, *18*, 621.
(15) Liao, H. G.; Zheng, H. M. *J. Am. Chem. Soc.* **2013**, *135*, 5038.
(16) Mueller, C.; Harb, M.; Dwyer, J. R.; Miller, R. J. D. *J. Phys. Chem. Lett.* **2013**, *4*, 2339.
(17) Yuk, J. M.; Park, J.; Ercius, P.; Kim, K.; Hellebusch, D. J.; Crommie, M. F.; Lee, J. Y.; Zettl, A.; Alivisatos, A. P. *Science* **2012**, *336*, 61.
(18) Liao, H. G.; Cui, L. K.; Whitelam, S.; Zheng, H. M. *Science* **2012**, *336*, 1011.
(19) Li, D. S.; Nielsen, M. H.; Lee, J. R. I.; Frandsen, C.; Banfield, J. F.; De Yoreo, J. J. *Science* **2012**, *336*, 1014.
(20) Chen, Q.; Smith, J. M.; Park, J.; Kim, K.; Ho, D.; Rasool, H. I.; Zettl, A.; Alivisatos, A. P. *Nano Lett.* **2013**, *13*, 4556.
(21) Zheng, H. M.; Claridge, S. A.; Minor, A. M.; Alivisatos, A. P.; Dahmen, U. *Nano Lett.* **2009**, *9*, 2460.
(22) Kelley, E. G.; Albert, J. N. L.; Sullivan, M. O.; Epps, I. I. I. T. H. *Chem. Soc. Rev.* **2013**, *42*, 7057.
(23) Brodin, J. D.; Ambroggio, X. I.; Tang, C.; Parent, K. N.; Baker, T. S.; Tezcan, F. A. *Nat. Chem.* **2012**, *4*, 375.
(24) Doncom, K. E. B.; Hansell, C. F.; Theato, P.; O'Reilly, R. K. *Polym. Chem.* **2012**, *3*, 3007.
(25) Xing, Z.; Zhang, J.; Li, X.; Zhang, W.; Wang, L.; Zhou, N.; Zhu, X. *J. Polym. Sci. A1* **2013**, *51*, 4021.
(26) Jiang, J.; Tong, X.; Zhao, Y. *J. Am. Chem. Soc.* **2005**, *127*, 8290.
(27) Ren, H.; Wu, Y.; Ma, N.; Xu, H.; Zhang, X. *Soft Matter* **2012**, *8*, 1460.
(28) Lensen, D.; Gelderblom, E. C.; Vriezema, D. M.; Marmottant, P.; Verdonschot, N.; Versluis, M.; de Jong, N.; van Hest, J. C. M. *Soft Matter* **2011**, *7*, 5417.
(29) Chien, M.-P.; Rush, A. M.; Thompson, M. P.; Gianneschi, N. C. *Angew. Chem., Int. Ed.* **2010**, *49*, 5076.
(30) Ku, T.-H.; Chien, M.-P.; Thompson, M. P.; Sinkovits, R. S.; Olson, N. H.; Baker, T. S.; Gianneschi, N. C. *J. Am. Chem. Soc.* **2011**, *133*, 8392.
(31) Hoppe, S. M.; Sasaki, D. Y.; Kinghorn, A. N.; Hattar, K. *Langmuir* **2013**, *29*, 9958.
(32) Plamper, F. A.; Gelissen, A. P.; Timper, J.; Wolf, A.; Zezin, A. B.; Richtering, W.; Tenhu, H.; Simon, U.; Mayer, J.; Borisov, O. V.; Pergushov, D. V. *Macromol. Rapid Commun.* **2013**, *34*, 855.
(33) Xia, Y.; Olsen, B. D.; Kornfield, J. A.; Grubbs, R. H. *J. Am. Chem. Soc.* **2009**, *131*, 18525.
(34) LaGrange, T.; Campbell, G. H.; Reed, B. W.; Taheri, M.; Pesavento, J. B.; Kim, J. S.; Browning, N. D. *Ultramicroscopy* **2008**, *108*, 1441.
(35) Kim, J. S.; Lagrange, T.; Reed, B. W.; Taheri, M. L.; Armstrong, M. R.; King, W. E.; Browning, N. D.; Campbell, G. H. *Science* **2008**, *321*, 1472−1475.
(36) Evans, J. E.; Browning, N. D. *Microscopy* **2013**, *62*, 147−156.
(37) White, E. R.; Mecklenburg, M.; Shevitski, B.; Singer, S. B.; Regan, B. C. *Langmuir* **2012**, *28*, 3695.
(38) Woehl, T. J.; Park, C.; Evans, J. E.; Arslan, I.; Ristenpart, W. D.; Browning, N. D. *Nano Letters* **2013**, DOI: 10.1021/nl4043328.